AD-A039 753   WASHINGTON UNIV SEATTLE APPLIED PHYSICS LAB   F/G 8/12
                HIGH RESOLUTION OBSERVATIONS OF UNDER-ICE MORPHOLOGY,(U)
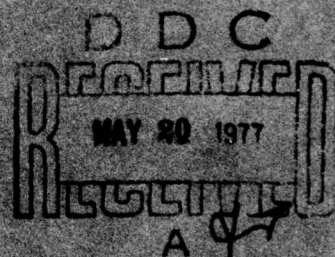   MAR 77   R E FRANCOIS   N60921-76-M-6536
UNCLASSIFIED   APL-UW-7712   NL

1 OF 1
ADA039 753

END

DATE
FILMED

6-77

HIGH RESOLUTION OBSERVATIONS OF UNDER-ICE MORPHOLOGY

APPLIED · PHYSICS · LABORATORY
A DIVISION OF THE UNIVERSITY OF WASHINGTON

HIGH RESOLUTION OBSERVATIONS OF UNDER-ICE MORPHOLOGY

by

Robert E. Francois

D D C

RECEIVED

MAY 20 1977

A

REPORT DOCUMENTATION PAGE		READ INSTRUCTIONS BEFORE COMPLETING FORM
1. REPORT NUMBER	2. GOVT ACCESSION NO.	3. RECIPIENT'S CATALOG NUMBER
4. TITLE *(and Subtitle)* High Resolution Observations of Under-Ice Morphology		5. TYPE OF REPORT & PERIOD COVERED
		6. PERFORMING ORG. REPORT NUMBER APL-UW-7712
7. AUTHOR(s) Francois, Robert E.		8. CONTRACT OR GRANT NUMBER(s) PO #N60921-76-M-6536
9. PERFORMING ORGANIZATION NAME AND ADDRESS Applied Physics Laboratory University of Washington 1013 N.E. 40th Seattle, WA 98105		10. PROGRAM ELEMENT, PROJECT, TASK AREA & WORK UNIT NUMBERS
11. CONTROLLING OFFICE NAME AND ADDRESS Naval Surface Weapons Center White Oak, Silver Spring, Maryland 20910		12. REPORT DATE 31 March 1977
		13. NUMBER OF PAGES 30
14. MONITORING AGENCY NAME & ADDRESS*(if different from Controlling Office)*		15. SECURITY CLASS. *(of this report)* Unclassified
		15a. DECLASSIFICATION/DOWNGRADING SCHEDULE

16. DISTRIBUTION STATEMENT *(of this Report)*

Approved for public release: distribution unlimited

17. DISTRIBUTION STATEMENT *(of the abstract entered in Block 20, if different from the report).*

18. SUPPLEMENTARY NOTES

19. KEY WORDS *(Continue on reverse side if necessary and identify by block number)*

Pressure ridge keel
Correlation of upper and lower ice surface
Void fraction

20. ABSTRACT *(Continue on reverse side if necessary and identify by block number)*

High resolution profiles of arctic under-ice topography were measured near Ice Island T-3, about 600 kilometers from the pole. A high frequency, narrow beam, profiling sonar carried by an unmanned, torpedo-like research submersible provided an ice elevation measurement each 38 cm along a guided path beneath the ice. Selected profiles that show normal, oblique, and nearly parallel traverses of pressure ridge keels are shown. Pressure ⟶

next page

DD FORM 1473 EDITION OF 1 NOV 65 IS OBSOLETE
1 JAN 73
S/N 0102-014-6601

031700

cont

ridges are shown to have block sizes of the dimensions of the parent ice
sheet.   The ridge keels have not consolidated into a homogeneous mass but
are replete with large voids and niches, and individual blocks are clearly
identified.   These properties were found on new, first-year ridges and on a
4 year old sheer ridge that was formed in ice about 5 meters thick.   There is
evidence that consolidation of the ridges to depths of the parent ice sheet is
rapid.   Little evidence of keel erosion is observed.

TABLE OF CONTENTS

LIST OF FIGURES

I. INTRODUCTION

Detailed knowledge of under-ice morphology, particularly in the Arctic Ocean, is of fundamental importance to underwater acoustics as well as other areas of scientific investigations such as the study of ice deformation mechanics and resulting effect on global climatology, transit by ship both through and under the sea ice, the development of cleanup techniques for dealing with under-ice oil spills, and off-shore resource development in the Arctic Ocean and surrounding area. This report presents observations on under-ice morphology based on high resolution acoustic measurements taken with a very narrow beam, upward-looking sonar system mounted in an unmanned, torpedo-like submersible. The measurements obtained by this technique are unique in that they provide more details on under-ice structure than any other method.

II. BACKGROUND

The Arctic Ocean is perennially covered with sea ice that averages about 3 m in thickness. Deformation of the ice, because of wind and current forces primarily, causes compressive, shear, and tension failures of the parent ice sheet. The compressive and shear failures result in the formation of pressure ridges that appear to the above-ice observer as great windrows of ice rubble. A corresponding rubble pile exists on the underside of the ice below the surface manifestation. These pressure ridges occur at frequent intervals, especially near the shore boundaries. Typical spacings between ridges range from a few hundred meters near shore to densities of one and one-half to two ridges per kilometer in the central Arctic Ocean.

The submerged portion of a pressure ridge is referred to as a keel, or a pressure ridge keel, and its size is generally characterized by a single measure, namely, its maximum depth. The shape and structure of these ridge keels are known largely from two types of observations: test holes drilled down through the ridges, and sonar (inverted fathometer) observations made from submerged submarines. The first type of observation is limited by the small number of drill holes that can be made in a deep ridge keel; the second by the beam width of the vertical-looking sonar and the standoff distance necessary to ensure vessel safety. Nevertheless, submarine records have been the basis for most of our knowledge about the under-ice profile. This report is written to present the more detailed observations of this Laboratory for general use by acousticians, engineers, and physical scientists.

III.   EXPERIMENTAL METHODS AND PRECISION ESTIMATES

The observations of the under-ice profile were made using the Unmanned
Arctic Research Submersible (UARS) system,[1,2] which was developed by this
Laboratory as part of an ARPA-sponsored arctic technology program. Briefly,
the system consists of an acoustic telemetry-controlled, torpedo-like vehicle
that can operate under the arctic ice while carrying acoustic and other re-
search instrumentation (Figure 1). An acoustic tracking system determines the
position of a tracking projector mounted on the UARS at 2-second intervals.
Within a typical 4-kilometer diameter operating area, the standard error of
the position measurement is about 15 cm relative to an established reference
baseline.

The vehicle dynamic controls play an important role in the measurement
process. The vehicle controls its depth within 7 cm, and pitch and roll are
controlled within 0.5° with 30-sec periods for all three functions. During
turns, slightly larger errors are incurred, but these damp out very rapidly
when straight running is resumed.

The multi-beam, upward-looking acoustic lens that is used to measure the
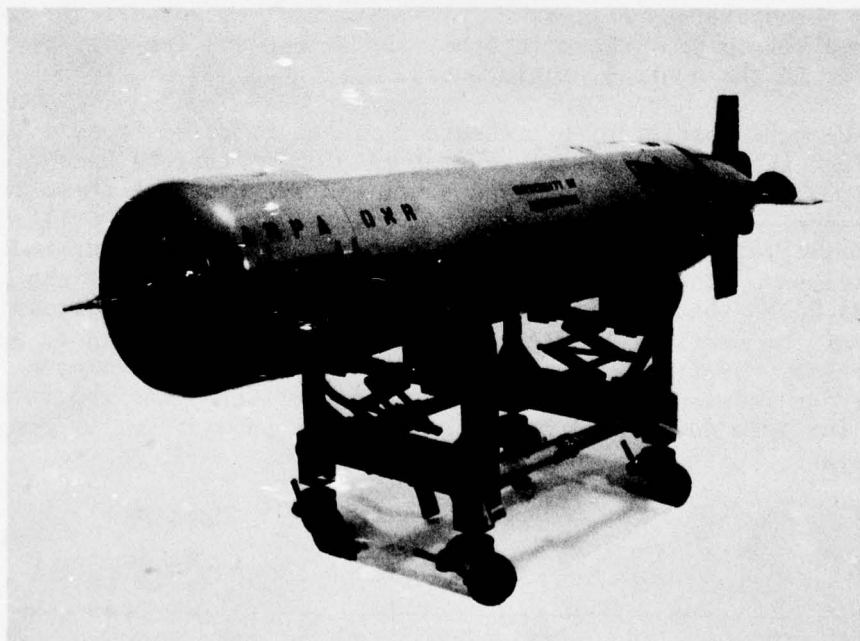under-ice profile is mounted directly over the tracking transducer (Figure 2).

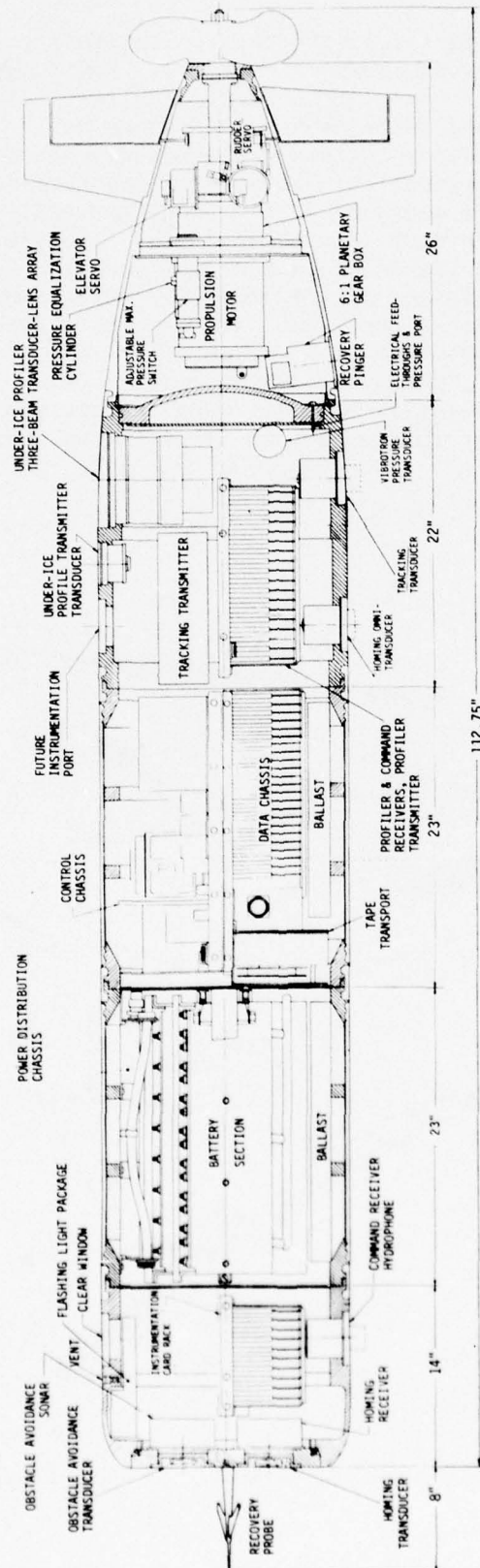*Figure 1.   UARS on Handling Dolly*

Figure 2. Cross-Sectional View of UARS

This report contains data taken with the zenith-looking acoustic beam only. The measurement geometry is shown in Figure 3. Measurement of the elevations z_{b1}, z_{b2},..., z_{bn} of the under-ice surface requires measurement of the distance from the sonar to the under-ice surface and sonar depth. The depth was derived from measurements of pressure with a precision Vibrotron® and water column density profile. Calibration for atmospheric pressure variations was made by correlating the distance measured by the acoustic profiler to the water surface of the launch/recovery hydrohole with the pressure measured by the vehicle sensor. The two-way sound transmission time was measured to the nearest 100 μsec. The water column velocity and density profiles were computed from CTD measurements made before and after each run. The composite standard error in absolute ice elevation under "flat" ice is 9 cm; possible errors arise from measurement of depth pressure, roll, pitch, two-way acoustic travel time to the reflecting surface, water column velocity profile, water column density, and quantization effects. The major contributor to this error is the quantization of sound travel time.
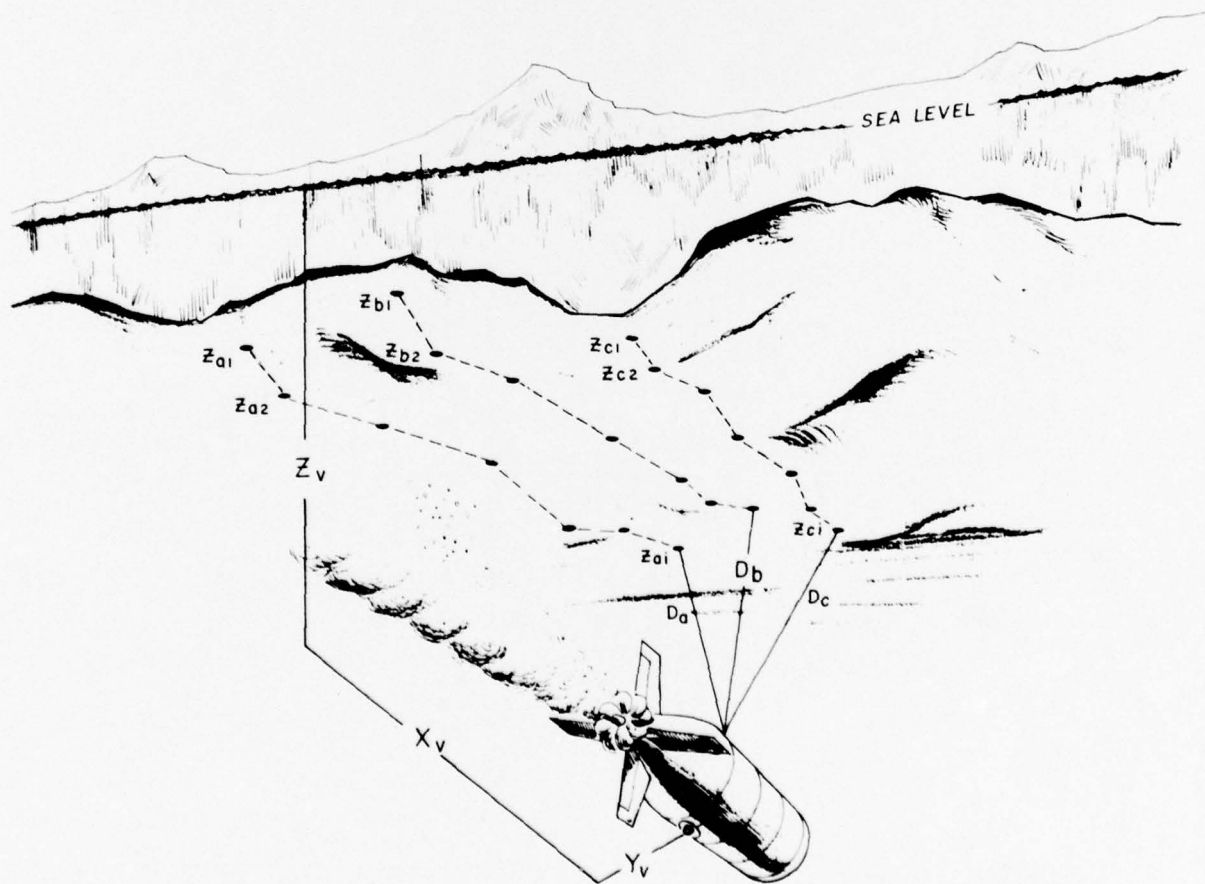

Figure 3. Measurement Geometry of UARS Profiling System

The beam width of the profiler transducer (the included angle between the half-power points) was 1° at 500 kHz. During the profile measurements presented in this report, the UARS was operating at a depth of 38 m. The "spot size" of the sonar beam was about 60 cm for most of the level ice under-run. The profiler measurements were made at a rate of 5 per second. The average velocity of the UARS during these measurements was 1.92 m/sec so that each "spot" overlapped its neighbor by about 56%.

When the reflecting surface of the ice is not normal to the acoustic beam, it is necessary to interpret the sonar distance measurement in a special way. If the signal ensonifies a surface with slope θ with respect to the acoustic wave front, the first reflected signal will arrive from the nearest part of the reflecting surface that is within the beam cone. The maximum difference in the range derived from this measurement and the true range to the constant slope surface at beam center is

$$\frac{B}{2} D \tan\theta,$$

where

B is the acoustic beam width (radians)
D is the separation distance between the sonar and reflecting surface
tan θ is the effective slope of the reflecting surface.

For a 30° sloping surface and 34 m range, the sonar will underestimate the correct range by approximately 17 cm. Corrections for this bias should be made when interpreting the data presented. Another way of looking at this effect is that the measured depth corresponds to a horizontal position that is biased toward the increasing depth by the corresponding half-beam-width distance.

A related problem is defining the physical and acoustic under-ice "surface" during ice accretion. Reflection of acoustic energy from the ice underside requires an acoustic impedance (ρc) mismatch between the water and ice, but the exact depth of effective acoustic penetration into the skeletal layer of the growing ice is unknown. Experimental evidence indicates, however, that this relatively unknown factor is small compared to the quantizing error.

IV. EXPERIMENTAL FIELD PROGRAM

The under-ice profiles presented here were obtained during a UARS field development program at Fletcher's Ice Island (T-3) during April and May of 1972. At that time, the island was essentially stationary near 84.5° north latitude and 84.5° west longitude. The location of the experimentation test site relative to T-3 is shown in Figures 4 and 5. As shown in Figure 4, an old shear ridge lay along a line more or less tangent to the island. Inside of this ridge lay Colby Bay, an area of unridged sea ice that had been fast to the island for approximately 8 years. The typical ice draft in the bay was 4 to 6 m. The refrozen lead identified in Figure 5 was not discernible to the eye.

Figure 5 shows the numbered sequence of 183° right turns made by the UARS. Changes in course of 30° were commanded near the center of the track, with a 15° change commanded halfway through the run so that subsequent runs would interleave. Since the run took over 4 hours, the effect of the earth's rotation can also be seen, although a major part of this effect was compensated for by the course gyro adjustment. The small loop in the center of the figure is the track of the UARS during its second pass at the homing beacon/recovery net during the homing phase. (This UARS trajectory plan was designed to support not only the under-ice profile measurements, but also another acoustic experiment related to forward scattering.[3])
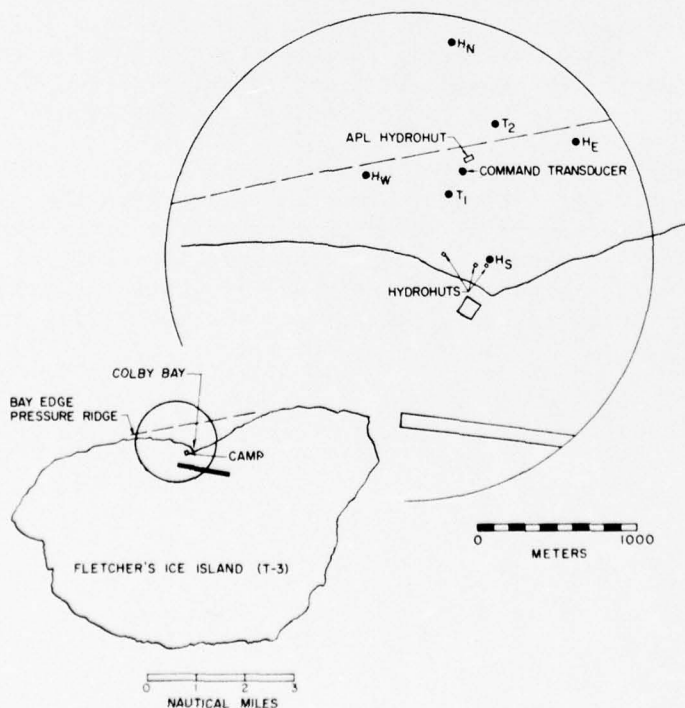

Figure 4. UARS System Geometry at Fletcher's Ice Island (T-3)

The position of UARS is computed from tracking information and is listed on a line printer, along with acoustic telemetered data from the vehicle. Launch and recovery were made through a hydrohole (1.2 x 3.6 x 8.5 m deep) made in the ice under the control building.[1,4]
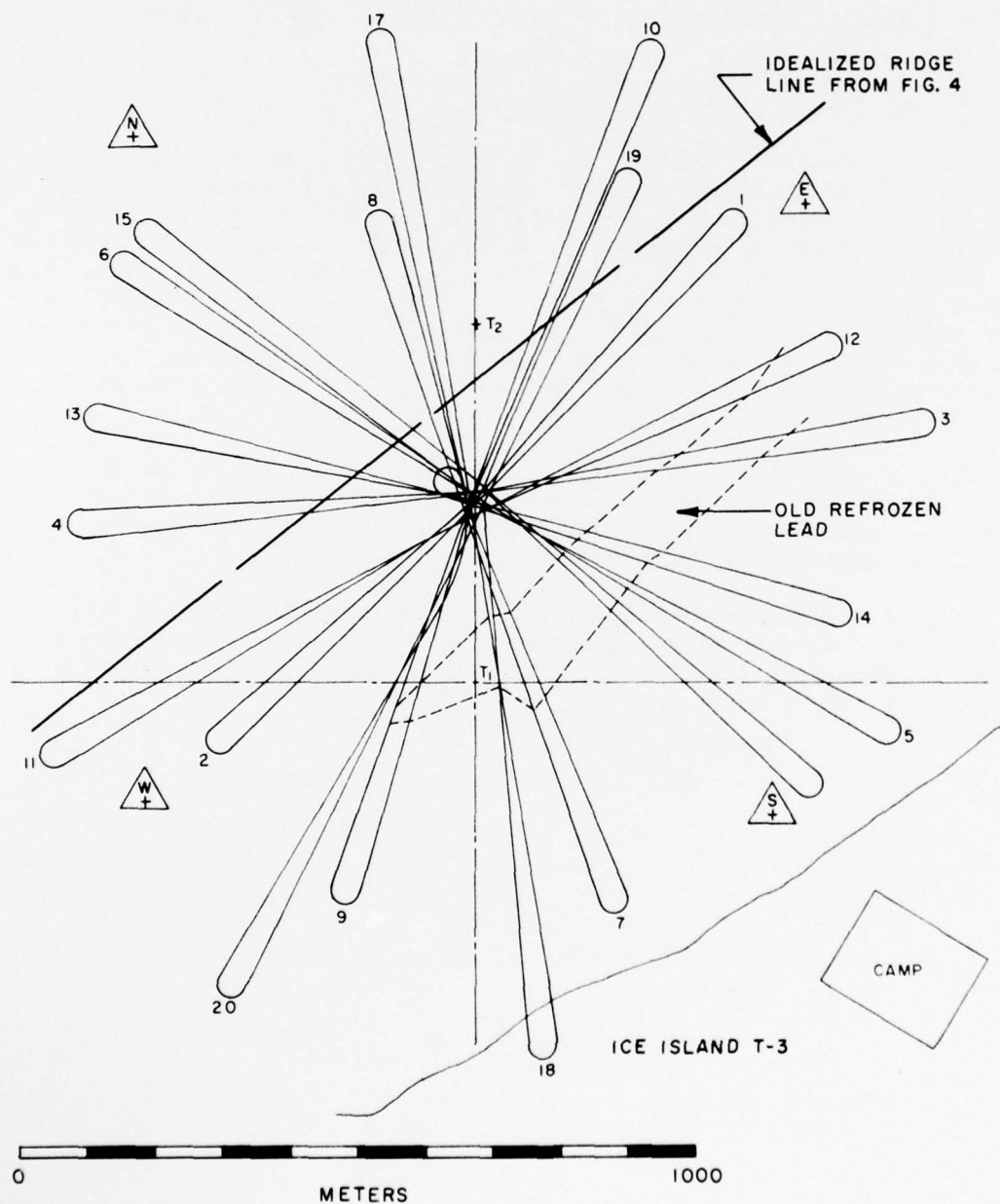

Figure 5. UARS Trajectory, 9 May 1972

V.   RESULTS

The profile measurements were recorded internally on the UARS with a spe-
cial digital recorder system that stored 1000 bits of data each second.   The
processed results are presented in graphical form in this report.

Correlation of Upper and Lower Ice Surface

The trajectory leg labeled 5-6 in Figure 5 was approximately normal to a
series of pressure ridges.   A level traverse was made across the corresponding
upper surface, using conventional surveying techniques.   Figure 6 combines the
under-ice elevation data from the center beam of the profiler and the ice sur-
face data from the level traverse.   The snow elevation is not shown.   Upper
surface measurements were made at 3 m intervals along the 1.3 km traverse.   The
lower surface is a digital lifted-pen plot of the profiler data, which includes
more than 4000 discrete measurements.   The traverse extends left-to-right, and
top-to-bottom from turn 5 to turn 6.   Note that the vertical-to-horizontal scale
ratio is 5 to 1.

The pressure ridge at the division of Colby Bay and the ice seaward of the
island was an old shear ridge with a well-rounded upper surface.   The remaining
ridges were first-year features with sharp ice blocks.   Drifting snow encased
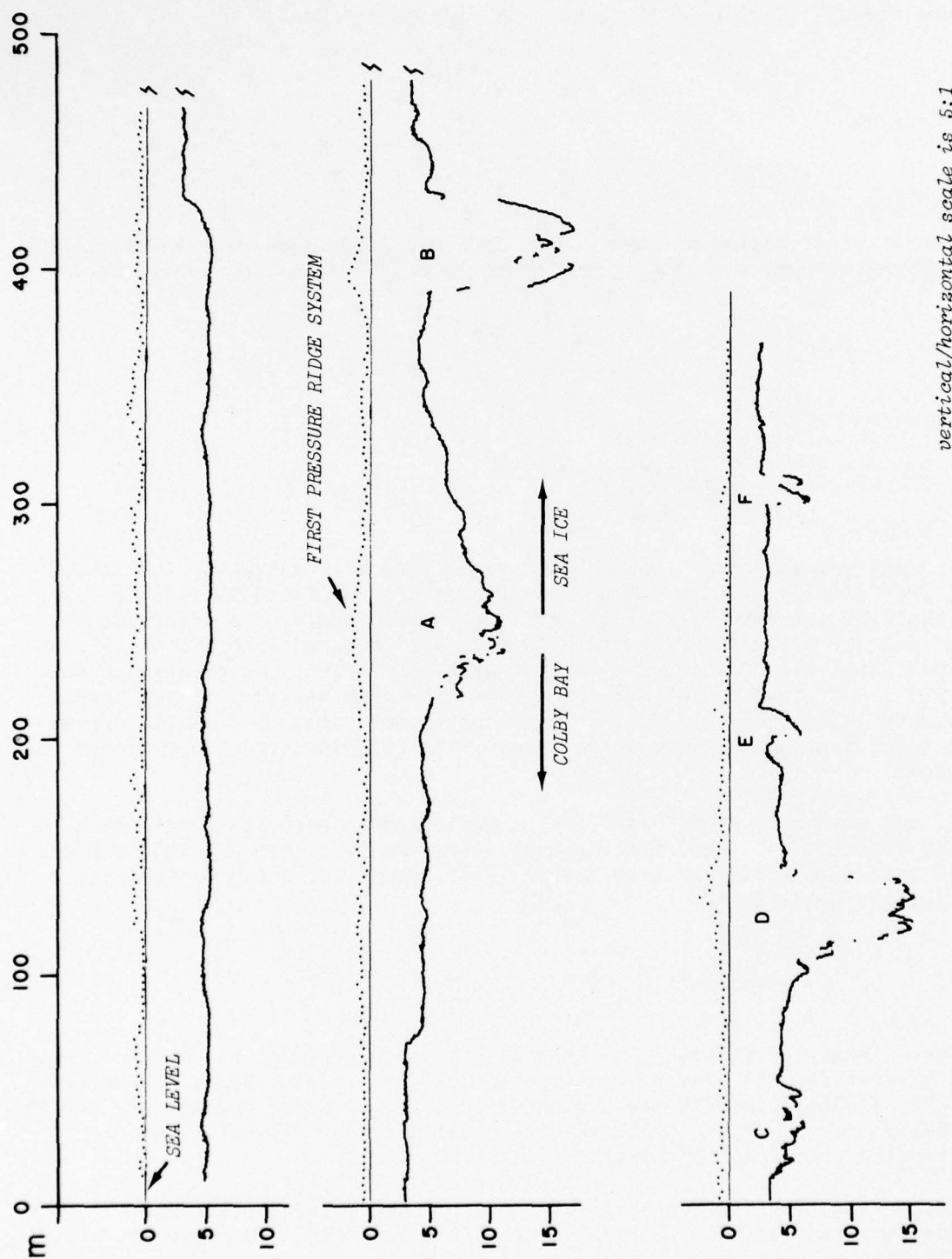most of the upper ridge features.

The ratio of maximum lower-ice surface elevations below sea level to the
maximum upper surface ice elevation associated with each ridge along the meas-
urement traverse is listed below.   Letters identifying each particular ridge
are shown in Figure 6.

$$
\begin{array}{rl}
A - & 8.60 \\
B - & 9.57 \\
C - & 8.33 \\
D - & 6.51 \\
E - & 5.61 \\
F - & 11.72
\end{array}
$$

Similar ratios based on maximum elevation of the snow surfaces at each
pressure ridge crossing are:

$$
\begin{array}{rl}
A - & 6.88 \\
B - & 9.25 \\
C - & 6.08 \\
D - & 5.97 \\
E - & 4.44 \\
F - & 5.32
\end{array}
$$

How close these ridges are to isostatic equilibrium can be determined by
correcting the observed upper-ice elevation for the snow overburden.   The snow

Figure 6. Upper and Lower Surface Profiles of Pressure-Ridged Ice taken during UARS Operation at Ice Island T-3

density was approximately half that of the sea ice; the corresponding ratio of pressure ridge keel depth to "equivalent" ridge elevation is:

A - 7.64
B - 9.41
C - 6.43
D - 6.23
E - 4.96
F - 7.56

These latter ratios average 7.03. If a pressure ridge were isostatically balanced throughout, with no voids, the ratio of the elevations would be

$$\frac{z}{h} = \frac{\rho_i}{\rho_w - \rho_i},$$ (1)

where

    z = ice elevation below sea level
    h = ice elevation above sea level
    ρ_i = density of the sea ice
    ρ_w = density of the sea water.

The sea water density, which was derived from CTD casts, was 1.0256 at depths from 6 to 30 m. The computed ratios of z/h for ice densities of 0.91, 0.90, and 0.89 are then 7.87, 7.16, and 6.56 respectively. An effective over-all ice density along the traverse of 0.9221 was computed from the digitized elevation data, the measured sea water density of 1.0256, and an assumed snow density one-half that of the sea ice. This is a best estimate of the actual ice density, since the void volume in the pressure ridges is a small portion of the total sectional volume considered. With this density, z/h is computed to be 8.91.

If one assumes that the ice (or ice equivalent) above sea level has a solidity fraction of x, and the ice keel below sea level has a solidity frac-tion of y (due to formation from broken ice blocks), Eq. 1 can be modified to reflect these conditions.

$$\frac{z}{h} = \frac{y\rho_i}{x(\rho_w - \rho_i)}$$ (2)

The solidity coefficient in the pressure ridge keel can be computed from Eq. 2 by inserting the previously computed ice density of 0.9921, the water density of 1.0256 (from CTD measurements), and the observed average z/h for the six pressure ridges (7.03). The resulting solidity coefficient is 0.789; the corresponding void fraction portion is 0.211.

The correlation relationship for the upper and lower surface elevations has been computed for the 425 sets of elevation data shown in Figure 6. For ice thickness t, a linear regression line fit to the data gives

$$t = 2.37 + 6.30 \text{ "}f\text{"},$$

with a correlation coefficient of 0.716; and for ice draft d,

$$d = 2.37 + 5.30 \text{ "f"},$$

with a correlation coefficient of 0.653. "f" is the equivalent ice freeboard (1/2 snow depth + ice freeboard).

Figure 6 illustrates how the ice thickness varies with age. At the inner portion of Colby Bay, the "flat" ice thickness is greatest. Decreases in ice thickness identify ice failure events and reattachment of different ages of ice. For example, the refrozen lead in the upper right and middle left plot show the effect of a large crack and subsequent rehealing, but with thinner (perhaps a year younger) ice to seaward. Increasingly different ice floes can be observed, particularly in the lower figure. Ridges E and F are formed from large slabs of the parent ice sheet. The morphology of these ridges is best seen in Figure 7.

Detailed Morphology

Figures 7 through 19 present expanded scale views of selected under-ice features. The ratio of vertical to horizontal scale in these figures is 2.75 to 1 because of the digital plotter incremental step characteristics and the relative data resolution. The dashed line at the top of each profile section is a steering record signal, digitized at a 5/sec rate with a dropout each second. Its axis has been adjusted to correspond with the sea level position. The trace indicates three zones of rudder position corresponding to straight ahead, left and right turn. (Control is actually proportional.) An example of this can be seen in Figure 14B. The X-axis is a time plot with the appropriate distance scaled from tracking-time data. The vertical plotting scale resolution of the original full-size plot was 7 cm per increment; each incremental step was 0.010 inch.

In these figures, time increases to the right. The small inset figure identifies the corresponding section of the trajectory that applies to each profile. Note in Figure 7, for example, that the B and C sections are nearly parallel passes (displaced by about 35 m). The pressure ridge at the left of B and the right of C is the same ridge. All turns of the UARS were to the right, the diameter of the turning circle being 41.5 m.

Near-Normal Profile Sections

Near-normal profile sections are shown in Figures 7, 8A, 9B, and 10.

The features in Figure 7A,B are the same features identified in Figure 6 as B, C, D, E, and F. Notice the apparent vertical discontinuity in the profiles at several places. This indicates either a near-vertical surface or a backward-tilted ice block, which the profiler sonar cannot image. The surfaces of the ridges indicate that they are made up of a jumble of large ice fragments, with a great deal of roughness on the ridge underside.
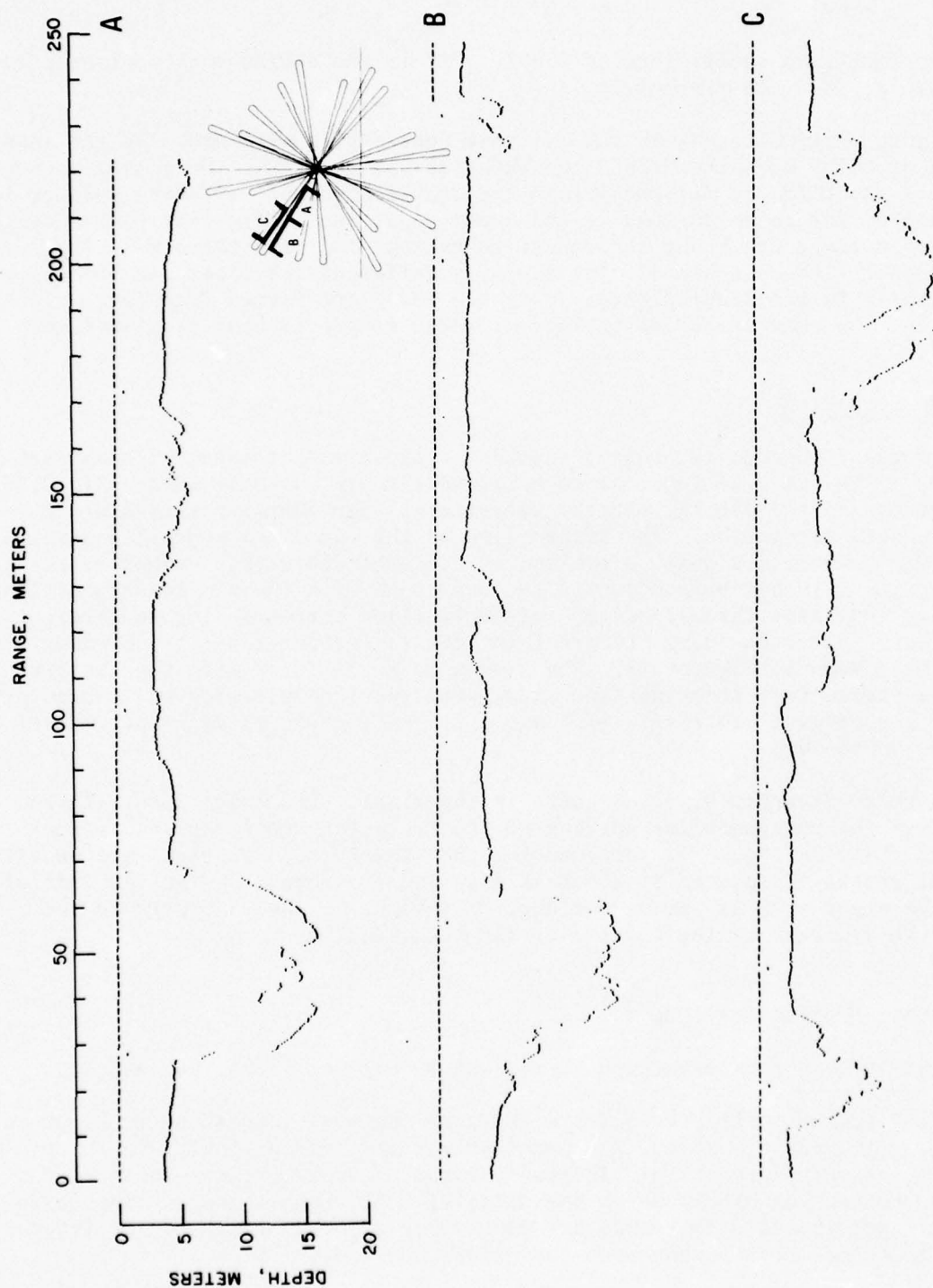
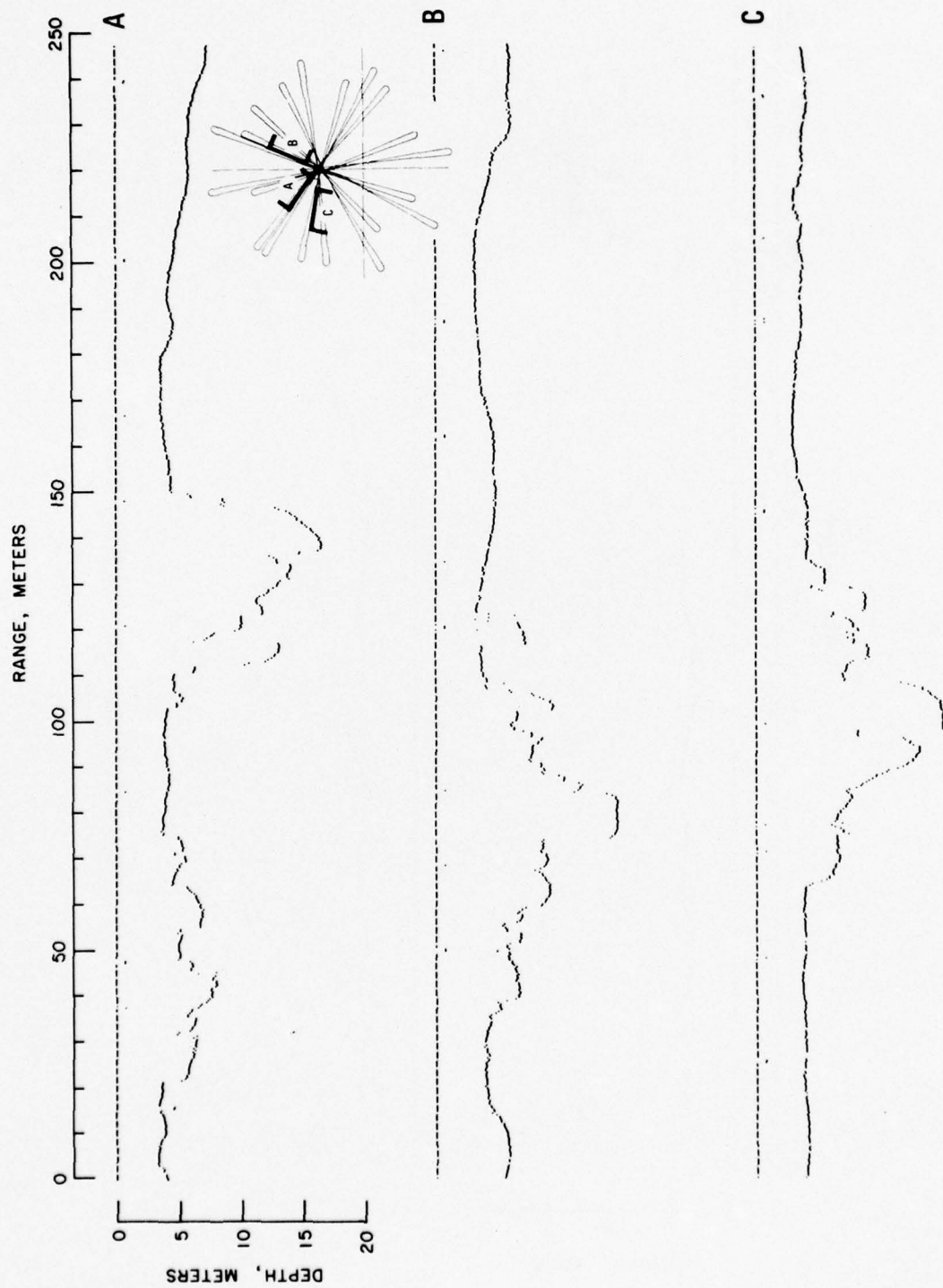Figure 7. Under-Ice Profile; Ridged Ice
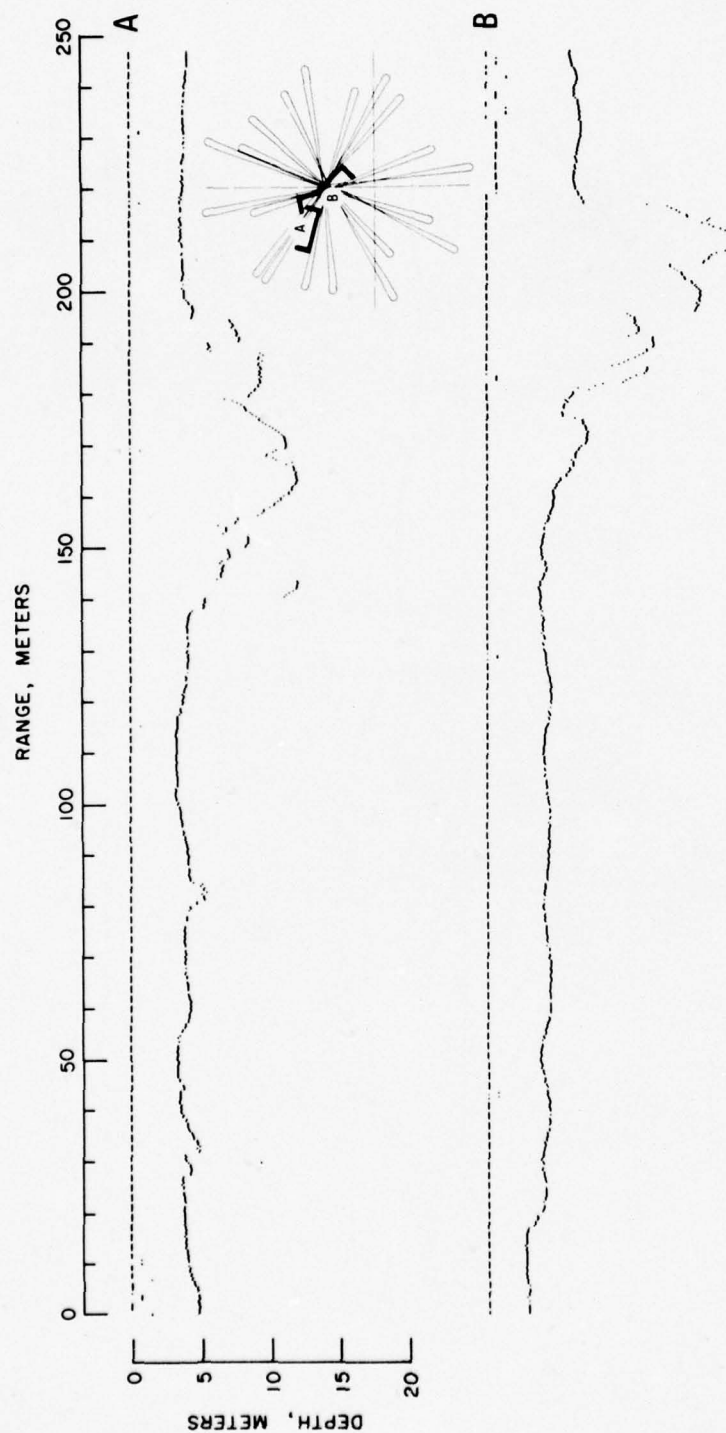
Figure 8. Under-Ice Profile; Ridged Ice
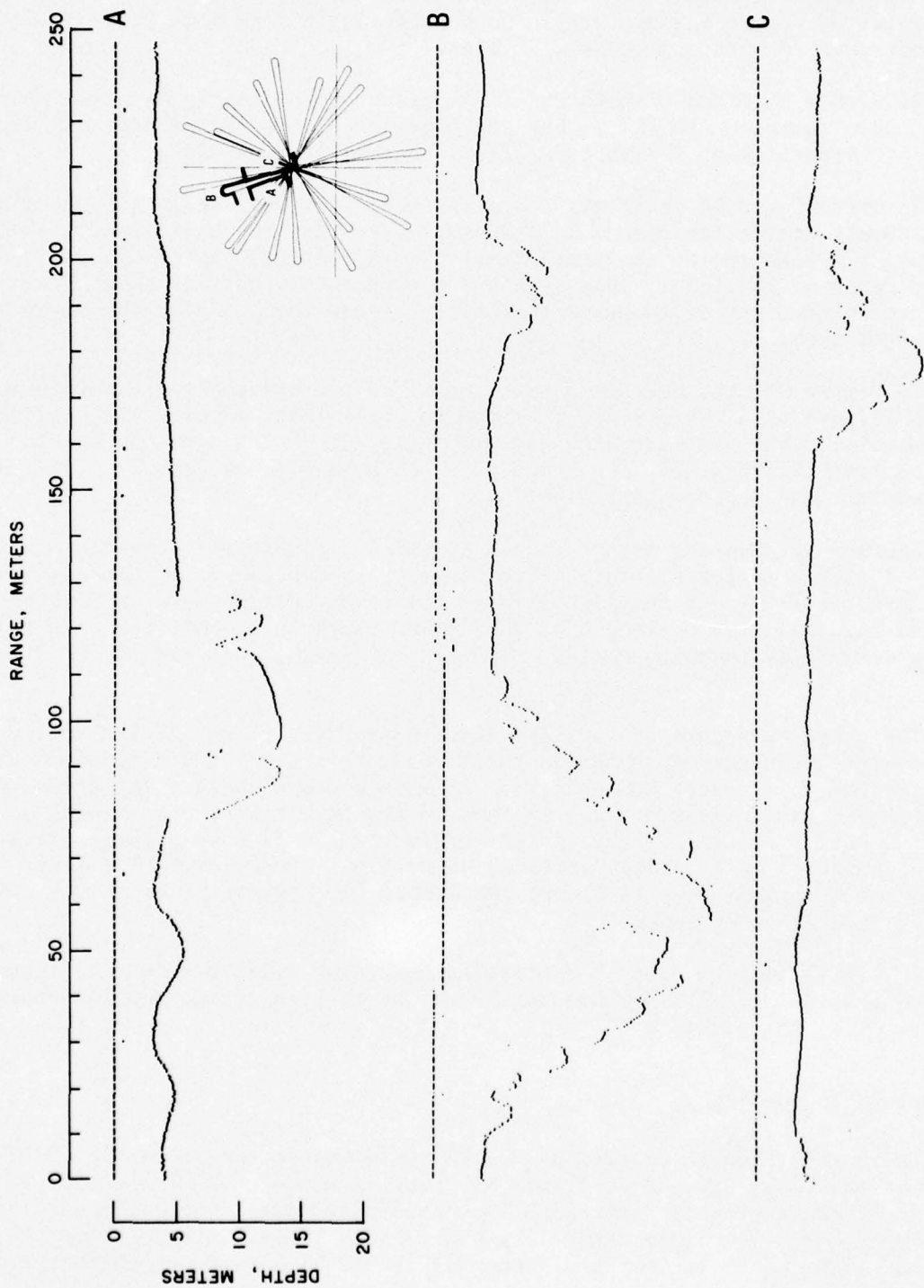
Figure 9. Under-Ice Profile; Ridged Ice

Figure 10. Under-Ice Profile; Ridged Ice

Figure 8A is a near parallel transit to Figure 7A, with a separation at the large ridge of about 20 m. The same feature (left side of ridge in Figure 7A, center of Figure 8A) appears in both profiles, giving some idea of the size of block that can make up pressure ridges.

In Figure 8, B and C appear at first glance to be nearly parallel profiles of the same feature. In fact, they are profiles of the same ridge, but with about 45° crossings at 90° to each other and separated by 400 m.

Figures 8C and 9A are nearly parallel profiles also--again separated by about 20 m. Notice the change in structure over this short distance. A unique feature is a slab of ice (to the left of the 9A feature) that is erected in a nearly vertical position. This slab has a parent thickness of about 3 m. A less prominent piece of the same thickness is seen about 6 m to the right of the deeper slab.

In Figure 9B, the feature shown is part of the old shear pressure ridge system (Figure 6A). This ridge is known to be at least 4 years old, and one can postulate that some rounding and smoothing has occurred due to erosion or new ice freezing; however, the ridge does not appear to be greatly different from newer ridges of the same size.

Another interesting set of ridges appears in Figure 10. The feature in Figure 10A is a tilted slab structure viewed in a canted plane, although the ridge profile is almost normal. This is the same ridge B shown in Figures 6, 7B, and 8A. The size or length of the intact blocks of parent ice is more easily visualized in this profile. The central block, for example, is 25 m long.

The ridge in Figure 10B was the deepest pressure ridge (22.3 m) observed in the area surveyed. As shown in the figure, this profile was measured while the UARS was in a turn. Consequently, it is not known whether the actual maximum depth of this pressure ridge is shown. The jumble of rubble making up this ridge is easily distinguished. In the center, there is a very large block. There appears to be an almost vertical niche 3 to 4 m wide and 10 m deep. A similar niche can be seen in Figure 10A also. The nominal slope of the ridge keel in Figure 10B is about 30°.

In Figure 10C, we again see a traverse through ridge B shown in Figures 6, 7B, 8A, and 10A. This ridge has dog-legged at this point and the 10C crossing is very close to normal.

Near-Parallel Profile Sections

The initial launch direction of UARS was almost parallel to the old shear ridge at the Colby Bay edge. Profile sections are shown in Figure 11. This section provides great insight into the uniformity or lack of uniformity of pressure ridge keels along their length dimension. Again, in spite of the age of this ridge, there is little evidence of the idealized shapes suggested by some modelers.[5,6]
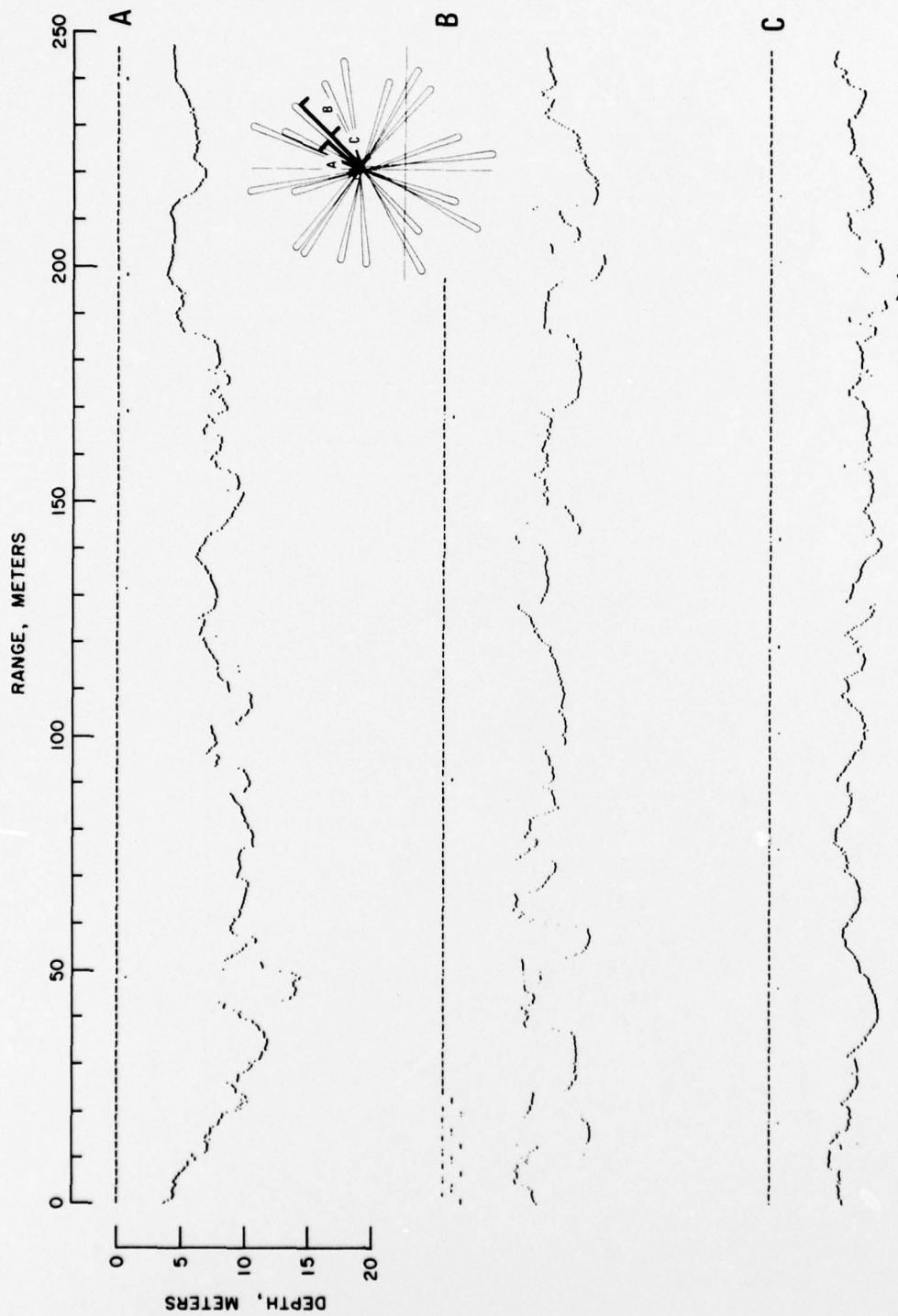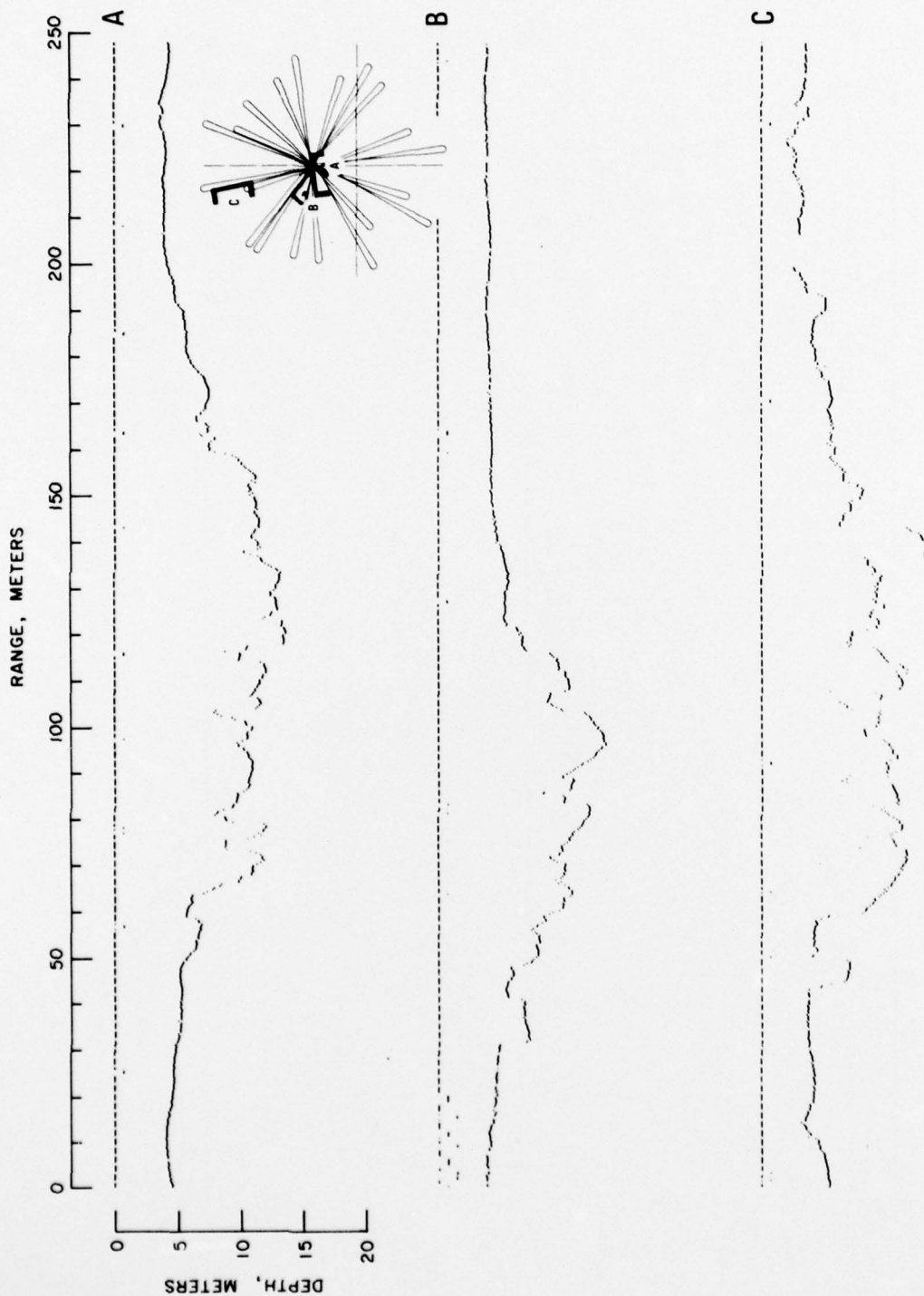
Figure 11. Under—Ice Profile; Ridged Ice.
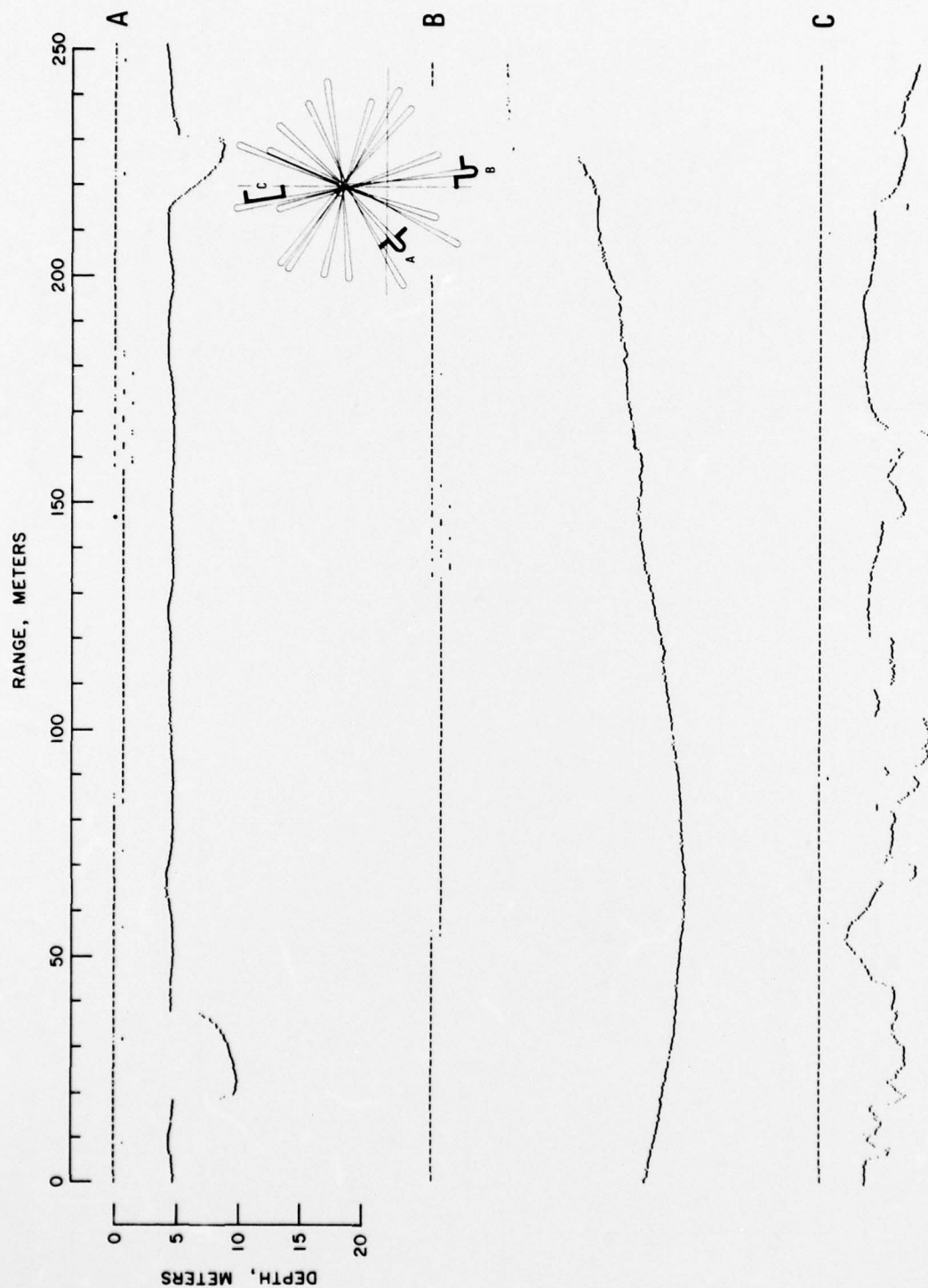
Figure 12. Under—Ice Profile; Ridged Ice

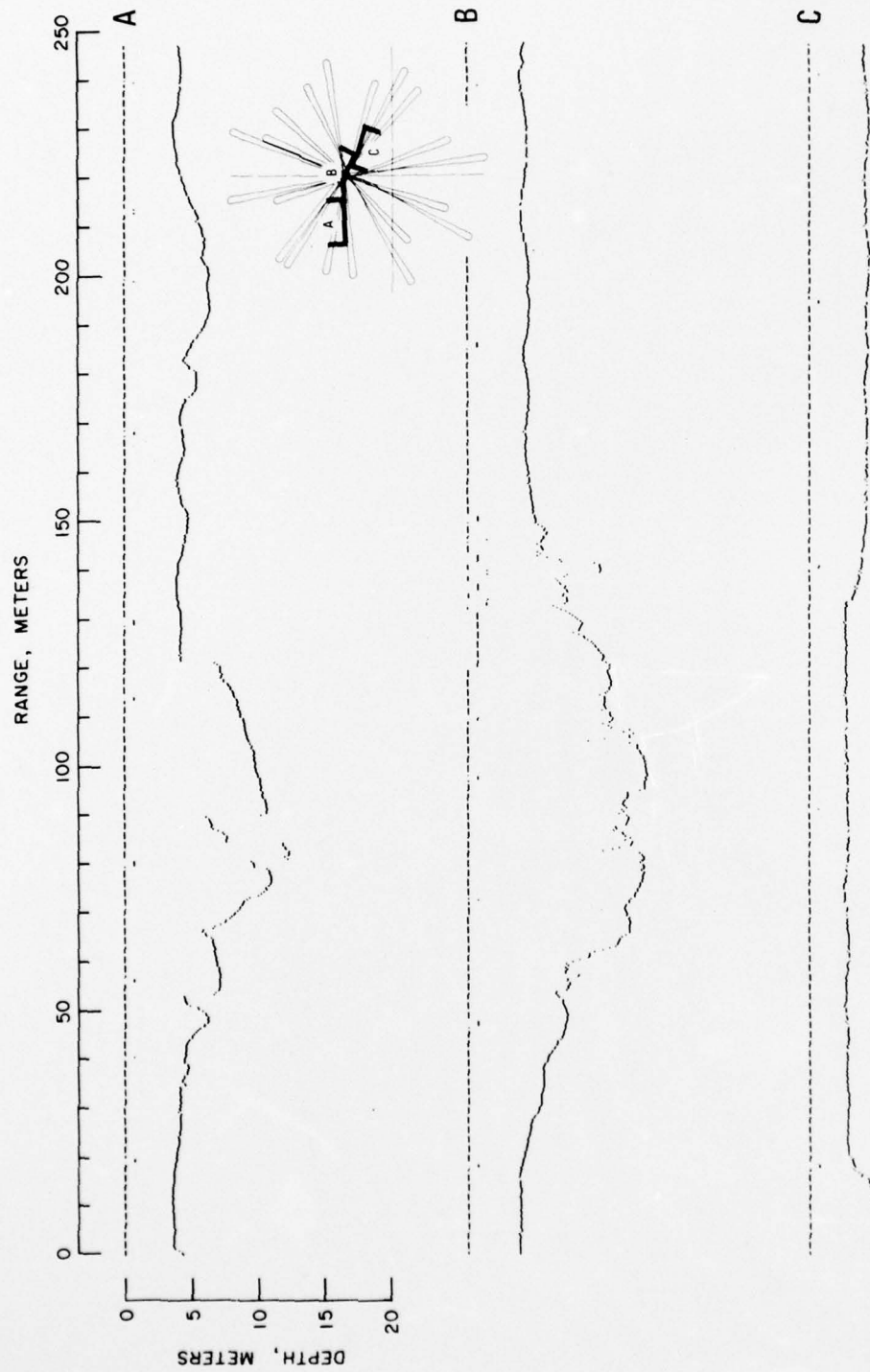Figure 13. Under-Ice Profile: Block in Lead; Under T-3; Hummock Field.

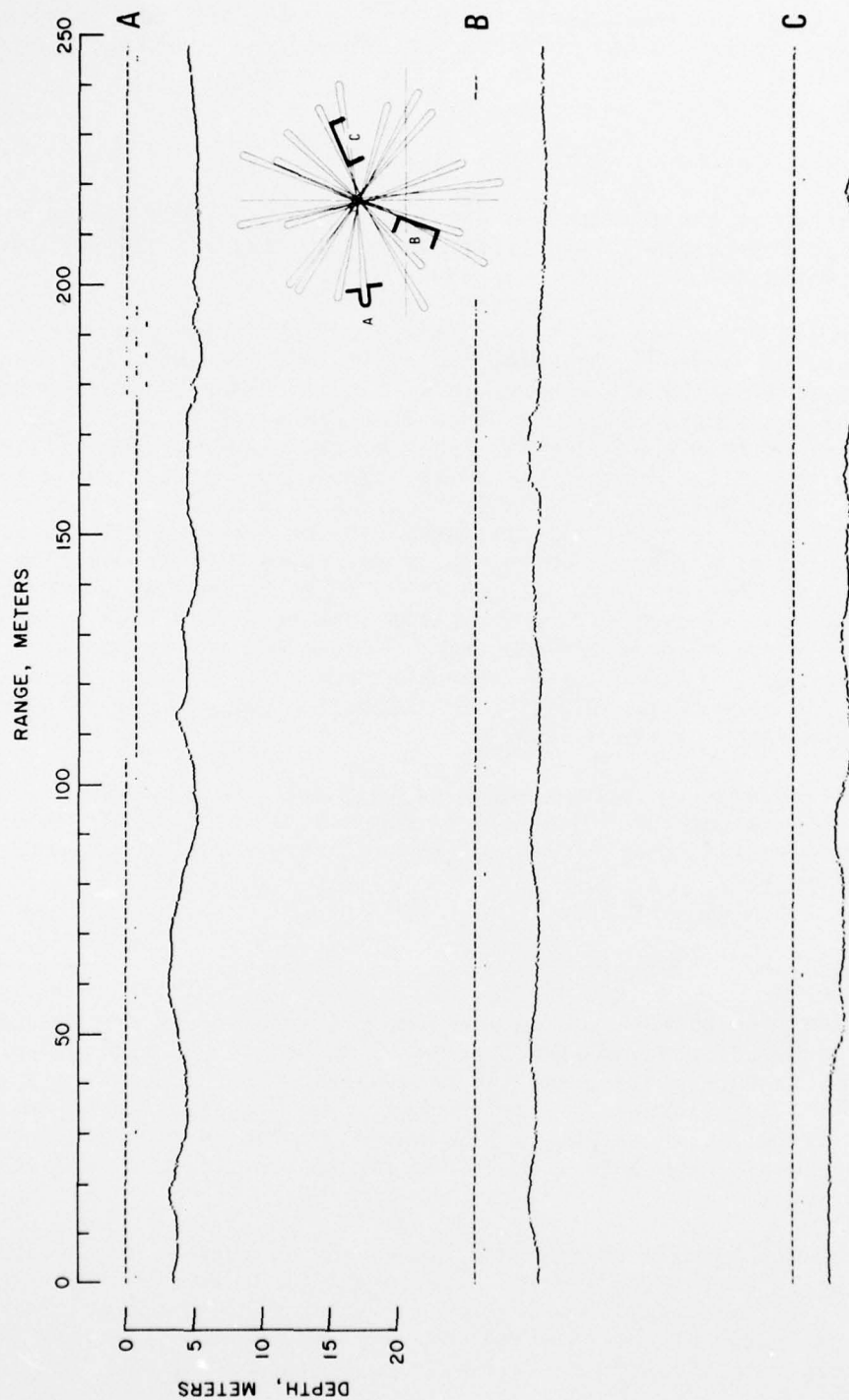Figure 14. Under-Ice Profile; Ridged Ice and Refrozen Lead

Figure 15. Under-Ice Profile; "Flat" Ice

Another nearly parallel traverse along a ridge keel is shown in Figures 12C and 13C. Judging from this group of measurements, we can safely conclude that the ice roughness characteristics along the long axis of pressure ridge keels are very similar to the characteristics observed in normal ridge crossings.

Oblique Profile Sections

In addition to the information contained in the oblique pressure ridge profile sections previously identified, additional insight is provided by Figures 12A,B and 14A,B.

Figures 12A,B and 14B show very clearly the phenomena reported in Zubov and attributed to Makarov[5] regarding deflection of the parent ice sheet in partially supporting the above water level rubble. Note the increasing draft of the parent ice sheets on both sides of the ridges in these figures. (These are keel sections from the old shear ridge previously described.) The apparent deflection noted in the figures is grossly excessive for the indicated thickness of ice. This deflection probably occurred when the ridge was formed years ago and the ice was substantially thinner. If the accretion of new ice was uniform in succeeding years, the initially deflected profile would be propagated to what we see here. If this is true, then the smoothing over of the pressure ridge keel itself by ice accretion must be a very slow process, for there is little evidence of the smoothing. Since the ice island (and presumably the attached ice floe) has been in the true central Arctic Ocean for many years, the slow rate of smoothing by ice accretion may generally apply to ridge keels throughout the Arctic Ocean.

A block longer than 30 m is included in the pressure ridge keel of Figure 14A. The remainder of the ridge keel is composed of much smaller blocks. Note the rough undersurface at the right of Figure 14A. A similar structure is noted in Figure 15A.

Refrozen Leads and "Flat" Ice

By "flat" ice, we mean ice on which no pressure ridges are discernible to the eye. However, for a variety of reasons, no sea ice is flat or smooth, particularly on its bottom side, and the unevenness of the ice bottom apparently increases with ice thickness or age (number of melt seasons experienced). An example of this is shown in Figure 14C, where the two ages of ice and corresponding roughness of the bottom are shown for an old refrozen lead and the adjacent older ice.

Much rougher terrain is shown in Figure 15. The profiles in Figure 15B,C are within Colby Bay, while the 15A profile was taken in sea ice outside the bay. A small refrozen lead can be seen in Figure 15B. A crack apparently formed in the center of the lead and thin ice was formed. When the ice came under pressure, the thinner ice failed and was extruded up and down to form a mini-ridge.
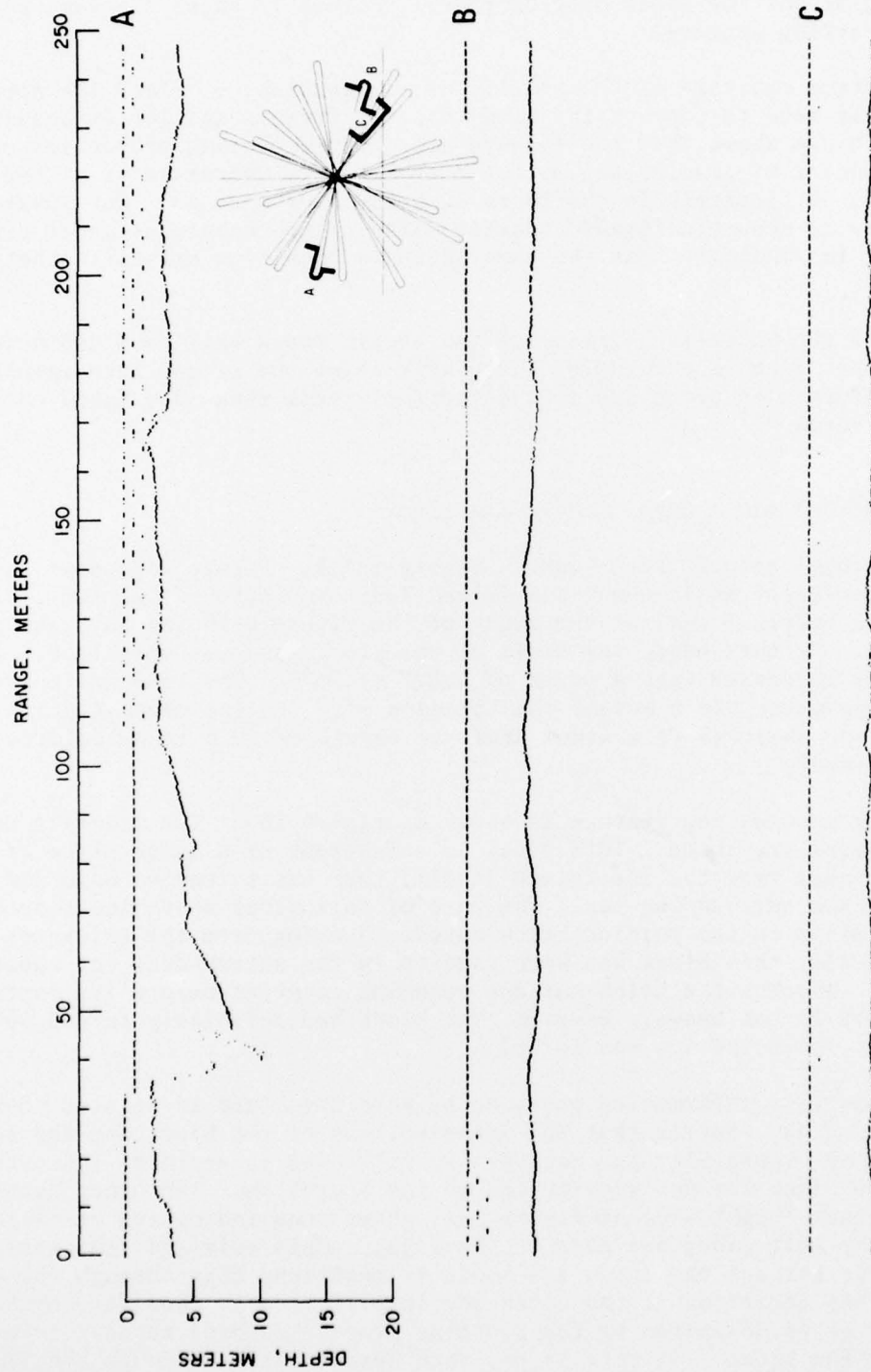
Figure 16. Under-Ice Profile; "Flat" Ice

A similar compression failure in the middle of a refrozen lead is shown in Figure 16A, but here some additional rafting apparently occurred. (Rafting is the sliding of one ice sheet over another.) Figure 17 shows the same phenomena again, in varying degrees.

A spectrum analysis of the profile of representative "flat" ice areas of Colby Bay was made to support the study made of forward scatter of acoustic energy.[3] It was shown that the forward acoustic reflecting properties of ice were independent of grazing angle, but correlated to the waviness of the under-ice surface, particularly in the 20 to 40 m wavelength range. Our subsequent measurements of acoustic forward scatter using other techniques under first and second year ice indicate that the same waviness condition exists in that ice also.[7]

Most of the under-ice surface of the Arctic Ocean will have characteristics more like the "flat" ice examples given here since the ridged area resulting from the deformation processes is substantially less than 50%, based on ridge density research.[5,8]

Under-run of T-3 and a Large Single Ice Block

Two unique features are shown in Figure 13A,B. Figure 13B shows the profile of a partial transit under Ice Island T-3. The edge of the ice island appears as a vertical wall at the right of the figure with the adjacent ice 6.5 m thick. At this edge, the draft of the ice island was only 12 m. The draft slowly increased with a slope of 0.027 (1.56°). The UARS was turned back after probing about 150 m beyond the island's edge, so the deepest draft of the island was not observed (a maximum draft in excess of 50 m is calculated for this ice island).

Another interesting feature is shown in Figure 13A. Two transits under a large ice block are shown. This block is a fragment of a large piece of ice (probably broken from the ice island itself) that has turned on edge and is frozen into the surrounding ice. The part of this block above ice showed rounding similar to the portion below water. Judging from the thickness of the surrounding ice, this block has been captive in the surrounding ice sheet for many years. Whether the below-surface rounding occurred before its capture in the ice sheet is not known. However, the block had definitely turned 90° from the plane in which the ice was formed.

The important information provided by this structure is related to the ice accretion process. Notice that the intersections of the block and the ice sheet (left of Figure 13A) are square. No filleting is visible, indicating that the ice block was not growing due to ice accretion. The other transit under the block (right side of Figure 13A) shows some indication of filleting action on the left side, but none on the right. This evidence indicates that heat transfer through the large ice block is much less than through the adjacent ice. Any accretion at the block-ice intersection is therefore either insignificant or is dominated by the freezing process related to heat transfer through the ice sheet. If this is so, then heat transfer through the jumble
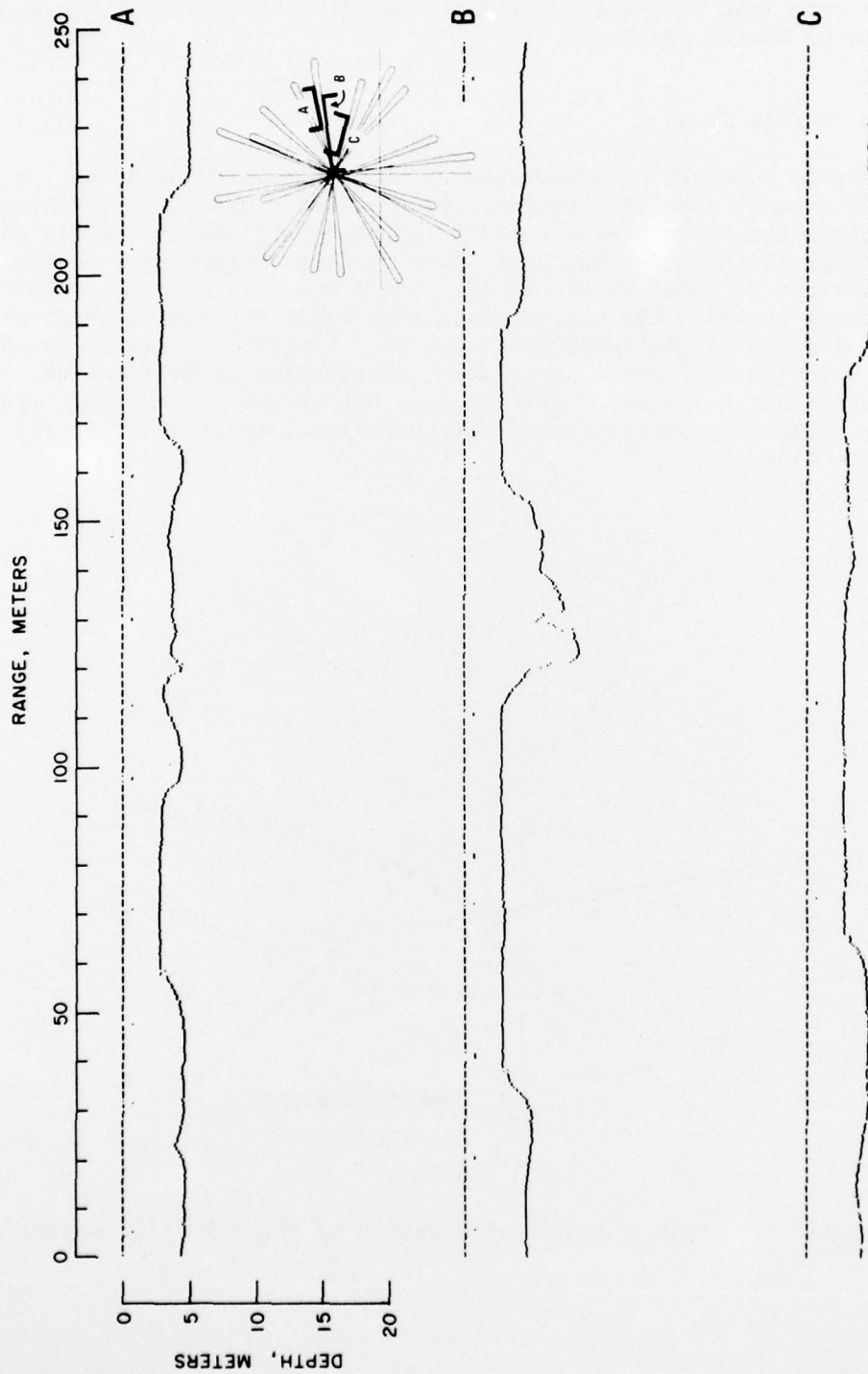
Figure 17. Under-Ice Profile; Ridge Formation in Refrozen Lead

of ice blocks below the level of the surrounding ice in pressure ridges must be very low; hence any consolidation of such ridges into monolithic structures may occur over very long time spans. The ice sheet in which this block is captured is known to be over 6 years old.

Small Area Profile Study

To provide a better understanding of the variability of under-ice structure within a small area of a pressure ridge, the intersection of three profiles is presented. The pressure ridge in these profiles is the old shear pressure ridge at the Colby Bay edge. The plan trajectory view of the three profile sections is shown in Figure 18. The arrows indicate the UARS' direction of travel in which the measurements were made; the numbers indicate which turn is at the end of the respective runs (see Figure 5). Figure 19 shows the profiles, with the same arrow and number notation for identification. The profile intersections A, B, and C are shown on both Figure 18 and 19. Profiles 3 and 13 are oblique crossings of the pressure ridge, while 17 is nearly normal to the ridge line.
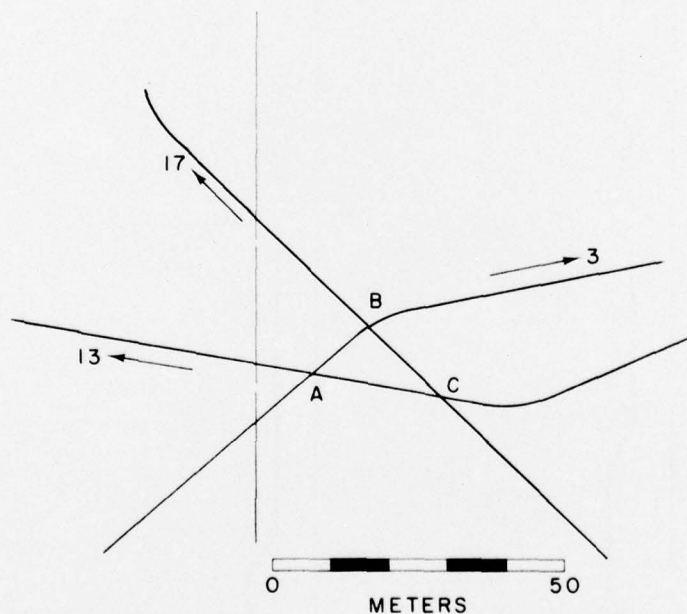

Figure 18. Plan View of Intersection of Three Profile Sections.
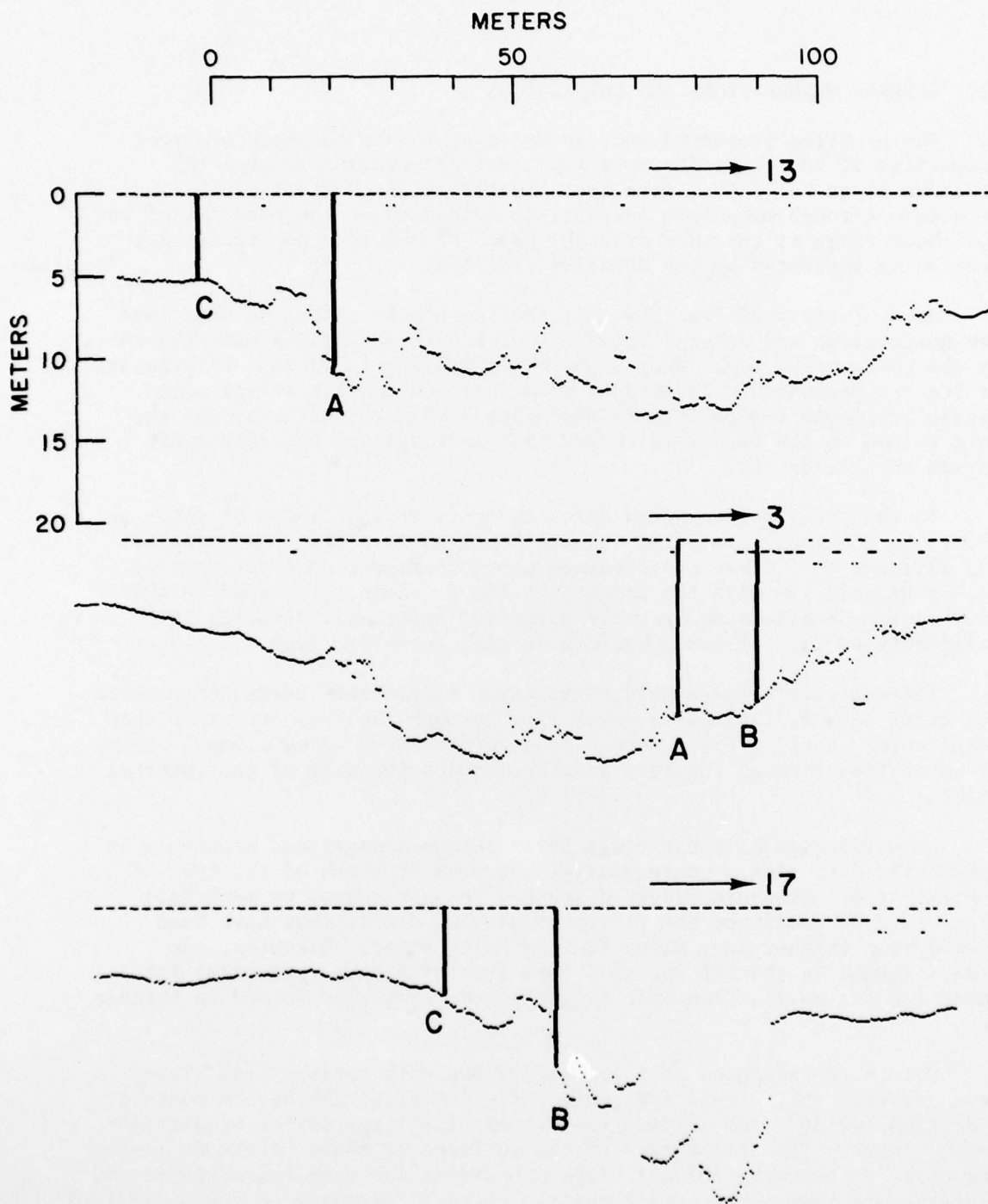
Figure 19. Three Intersecting Profiles

VI.   GENERAL OBSERVATIONS AND CONCLUSIONS

The profiles presented provide an insight into the morphological properties of sea ice. The most important observation is that the pressure ridge keels that were investigated retained their block-like structure through many melt seasons, as evidenced by the profiles of the old shear ridge at the edge of Colby Bay. No evidence of significant erosion is suggested by the detailed profiles.

Most of the profiles show that the ice blocks making up the ridge are quite large and consist primarily of blocks having the same thickness as the surrounding ice. Many examples of ridging in various thicknesses of ice are presented. Individual voids between the blocks are much larger in ridges formed from thicker rather than thinner ice, and the void volume in the former is larger than in ridges of the same draft formed in thinner ice.

In the profiles presented here, there is no indication of voids or niches in the keels closer to the sea level surface than the draft of the adjacent ice. Even newly formed pressure ridges show evidence of such consolidation with the parent ice sheet. Water entrapped in this zone cannot be displaced by small currents; apparently freezing is relatively rapid, following basic heat transfer principles.

The relatively large void cavities in ridge keels formed from thick ice offer less resistance to water flow through the keel structure than small voids in ridge keels formed from thinner ice. Even a small volume of water flow through the keel greatly impedes freezing of the internal voids.

Consolidation of these ridge keels into a homogeneous structure is apparently very slow. Consequently, the beam strength of the type of central Arctic pressure ridges discussed in this report is much less than would be predicted for ridges of similar drafts that have been formed from thinner ice, other factors being equal. Likewise, the ridges formed in thicker ice will form less effective cofferdams for under-ice oil spills than will ridges of the same size formed in thinner ice.

Only a few examples of a pressure ridge with classic side slopes were observed (see Figure 10B), and while one ridge did have a nominal side slope of 30°, the surface was formed of a large number of distinct large blocks. The orientation of the surfaces of these blocks is random and will dominate the nominal slope properties for many hydrodynamic and acoustic problems where length scales are small compared to the dimensions of the surface roughness.

VII. REFERENCES

1. R.E. Francois and W.E. Nodland, "Unmanned Arctic Research Submersible (UARS) System Development and Test Report," APL-UW 7219, Applied Physics Laboratory, University of Washington, Seattle, 11 September 1972.

2. R.E. Francois, "The Unmanned Arctic Research Submersible System," *Marine Technology Society Journal*, Vol. 7, No. 1, pp. 46-48.

3. R.E. Francois and W.E. Nodland, "Arctic Acoustic Measurements at 50 kHz," APL-UW 7313, Applied Physics Laboratory, University of Washington, Seattle, 31 August 1973.

4. R.E. Francois and J.G. Harrison, "A Thermal Drill for Making Large Holes in the Ice," *Ocean 75 Record*, Publication No. 75 CHO 995-1 OEC, The Institute of Electrical and Electronic Engineers, New York, N.Y. 10017.

5. W.I. Wittman and J.J. Schule, "Comments on the Mass Budget of the Arctic Ice Pack," In Proceedings of Symposium on the Arctic Heat Budget and Atmospheric Circulation, The Rand Corp. (RM-5233-NSF), 1966, pp. 217-246.

6. N.N. Zubov, *Arctic Ice*, Izdatel'stvo Glavsevmorputi, Moscow, 1943 (English Translation, AO 426 972, U.S. Navy Oceanographic Office, National Tech. Information Service, Springfield, Va.).

7. G.R. Garrison, E.A. Pence, and E.W. Early, "Acoustic Studies From an Ice Floe Near Barrow, Alaska, in April 1974," APL-UW 7514, Applied Physics Laboratory, University of Washington, Seattle, 29 February 1976.

8. T.L. Kozo and O.I. Diachok, "Spatial Variability of Topside and Bottomside Ice Roughness and its Relevance to Underside Acoustic Reflection Loss," AIDJEX Bulletin 79, University of Washington, Seattle, 1973, pp. 113-121.

ACKNOWLEDGEMENTS